

## Supporting Information

### Single-Nanowire Electrochemical Probe Detection for Internally Optimized Mechanism of Porous Graphene in Electrochemical Devices

*Ping Hu,<sup>‡</sup> Mengyu Yan,<sup>‡</sup> Xuanpeng Wang, Chunhua Han,\* Liang He, Xiujuan Wei, Chaojiang Niu, Kangning Zhao, Xiaocong Tian, Qiulong Wei, Zijia Li and Liqiang Mai\*.*

State Key Laboratory of Advanced Technology for Materials Synthesis and Processing, Wuhan University of Technology, Wuhan 430070, China

#### Corresponding Authors

\* E-mail: (L.M.) mlq518@whut.edu.cn.

\* E-mail: (C.H.) hch5927@whut.edu.cn.

## **Experimental**

### **1. Synthesis of MnO<sub>2</sub>, MnO<sub>2</sub>/rGO, and MnO<sub>2</sub>/pGO nanowires**

The MnO<sub>2</sub>/rGO nanowires were produced by the hydrothermal method. In a typical synthesis, 2 mmol KMnO<sub>4</sub>, 2 mmol NH<sub>4</sub>F and 2 ml of rGO suspension (~2 mg/ml) were added to 80 ml of distilled water and magnetically stirred at room temperature for 20 min. The sample was then placed into a 100 ml autoclave and heated at 180°C for 24 h. After the sample was washed and dried, a brownish-black powder was obtained. The pure MnO<sub>2</sub> nanowires were prepared using the same method described above without the addition of rGO. Then, we dealt MnO<sub>2</sub>/rGO with 10 mmol/L hydrazine hydrate for different times, including 1, 2, 3, 6, 12, and 24 hours. For improved structure and capacity over the different hydrazine hydrate MnO<sub>2</sub>/rGO nanowires, we chose to hydrate for 3 hours to produce the MnO<sub>2</sub>/pGO nanowires.

### **2. Structure Characterization**

X-ray diffraction (XRD) measurements were performed to investigate crystallographic information using a D8 Discover X-ray diffractometer with a non-monochromated Cu K $\alpha$  X-ray source. Field-emission scanning electron microscopic (FESEM) images were collected using a JSM-7001F microscope at an acceleration voltage of 10 kV. Transmission electron microscopic (TEM) and high-resolution TEM images were recorded with a JSM-2100F STEM/EDS microscope. The X-ray photoelectron (XPS) spectra were recorded on a Shimadzu Axis Ultra

spectrometer with an Mg  $K\alpha = 1253.6$  eV excitation source. An Autolab 302N Probe Station (Lake Shore, TTPX) and Semiconductor Characterization System (Agilent, B1500A) were used to test the electrochemical performances of the single-nanowire devices.

### **3. Fabrication of Single-Nanowire Electrochemical Devices**

Our manganese dioxide single-nanowire electrochemical device is configured with one single nanowire as a cathode, one flake of Au as an anode, and KOH (6 mol/L) as an electrolyte. The single-nanowire devices were fabricated by the following steps. EBL patterning of contact pads was performed on a highly doped silicon wafer with 300 nm  $\text{SiO}_2$ , followed by developing, rinsing, Cr/Au (5/50 nm) deposition by thermal evaporation, and then lift-off. The prepared  $\text{MnO}_2$  NWs were then deposited on the substrate by contacting the  $\text{MnO}_2$  nanowires and contact pad with Cr/Au electrode through EBL patterning, developing, rinsing, Cr/Au (5/150 nm) deposition by thermal evaporation, and then lift-off. A probe station was used for air characterization to check the I-V cyclic voltammetry performances of the  $\text{MnO}_2$  NWs. EBL patterning and developing of SU-8 2002 was used to create the isolation layer of the gold electrode to avoid leakage current. A drop of KOH (6 mol/L) electrolyte was used to coat the nanowire and the counter electrode (Au). The performance of the device was then tested. Furthermore, two other single-nanowire devices were fabricated by the same processes.

#### **4. Electrochemical Characterization**

For electrochemical characterization, the electrochemical performances of these single-nanowire electrochemical devices were measured by Autolab. The different single-nanowire electrochemical devices were fabricated using a mechanical shaping process modified from a previous method adopted to fabricate graphene-based, single-nanowire electrochemical devices. Electrochemical performances of the single-nanowire electrochemical devices were investigated in a two-electrode system using a cyclic voltammetry station and I-V properties. The scan rate of the CV response varied from 20 to 500 mV/s with a potential range from 0 to 0.8 V.

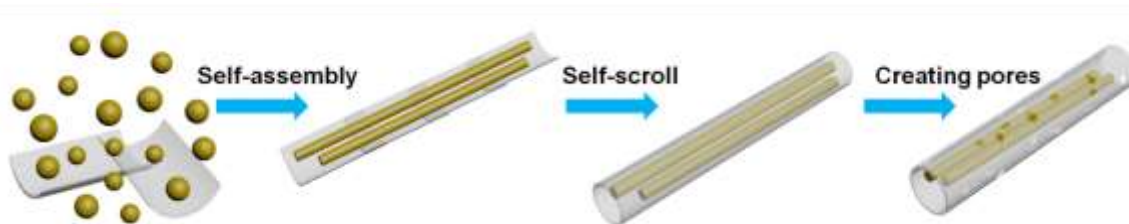


**Figure S1.** The construction processes of MnO<sub>2</sub>/pGO wire-in-scroll NWs. The brown dots represent the precursor of nanowire template, which forms the nanowires after hydrothermal processes. The gray sheets and scroll represent reduced graphene oxide.

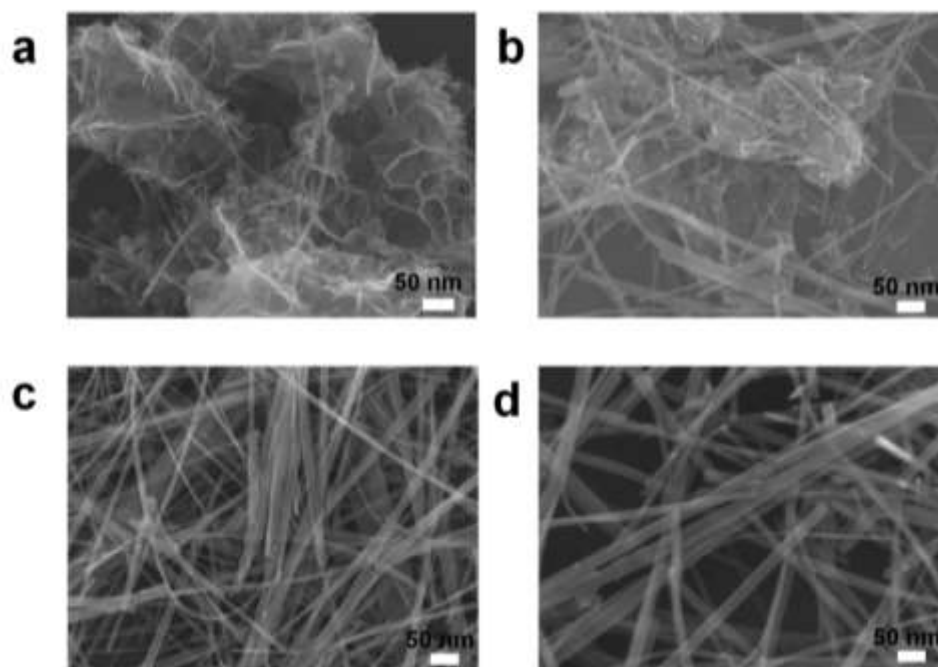


**Figure S2.** SEM images of different MnO<sub>2</sub>/rGO NWs produced by different hydrothermal times: (a) 3 h, (b) 6 h, (c) 12 h, (d) 18 h.

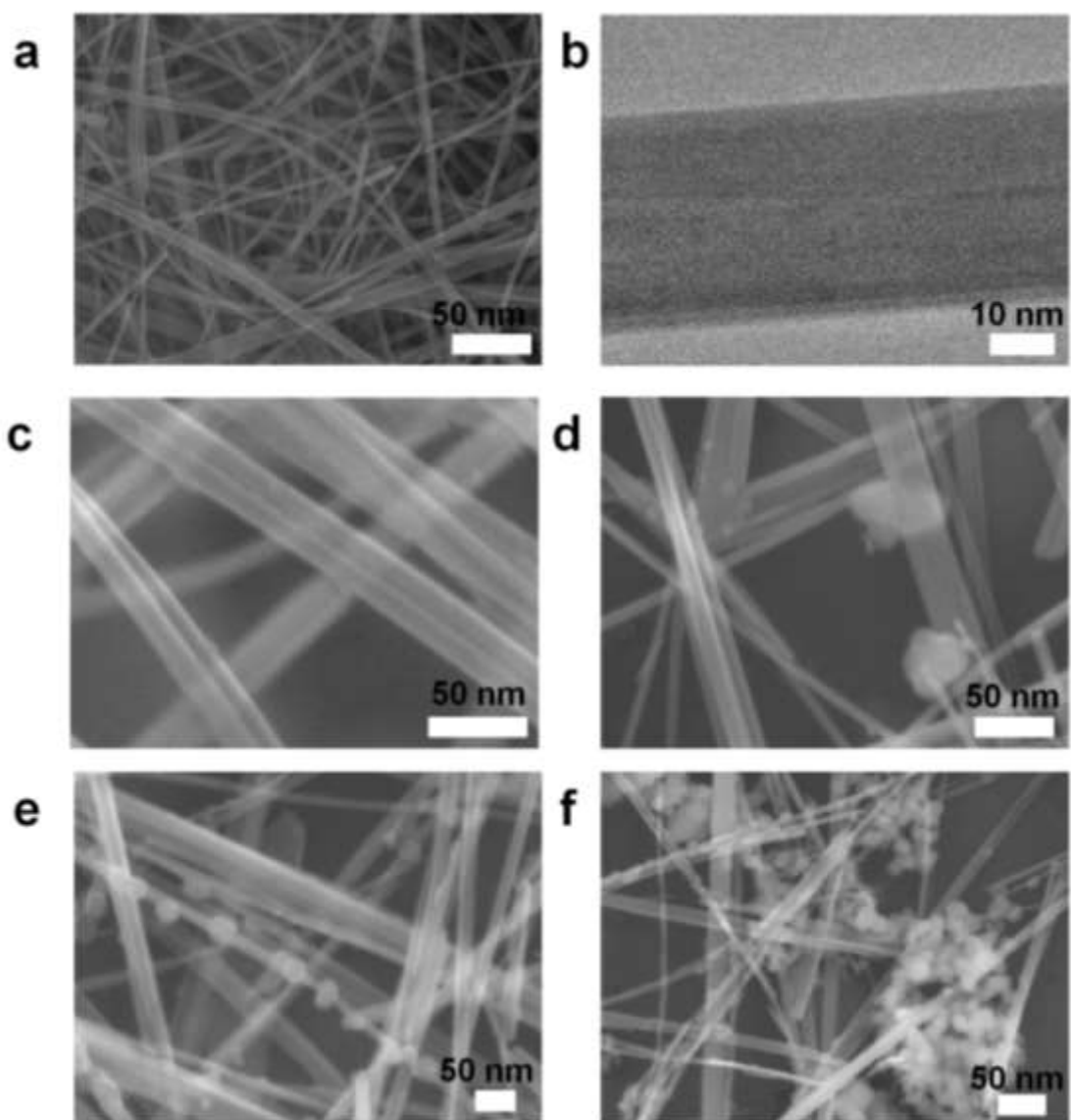


**Figure S3.** (a,b) SEM and TEM images of MnO<sub>2</sub>. (c) SEM image of MnO<sub>2</sub>/rGO. (d-f) SEM images of MnO<sub>2</sub>/rGO dealt with 10 mmol/L of hydrazine hydrate for different times: (d) 6h (MnO<sub>2</sub>-rGO-6h), (e) 12h (MnO<sub>2</sub>-rGO-12h), (f) 24 h (MnO<sub>2</sub>-rGO-24h).

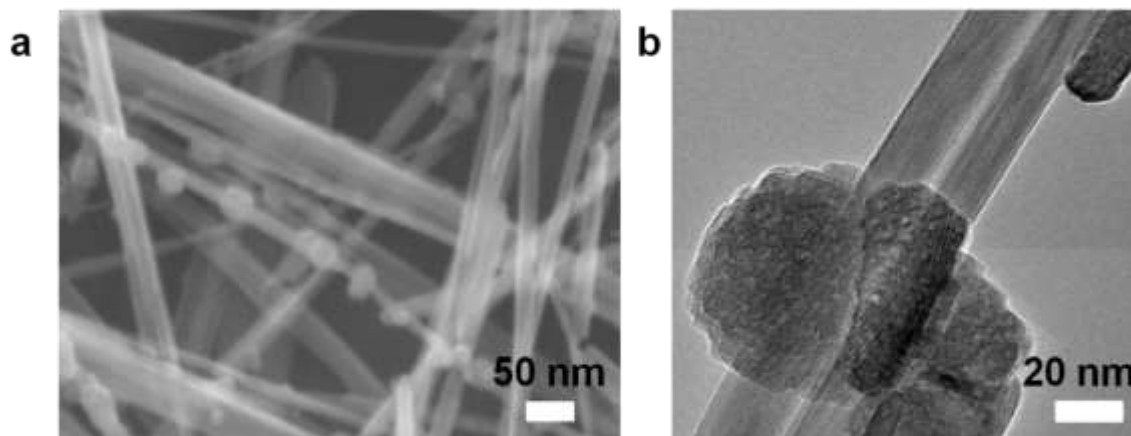


**Figure S4.** (a) SEM image of MnO<sub>2</sub>-rGO-12h. (b) TEM image of MnO<sub>2</sub>-rGO-12h.

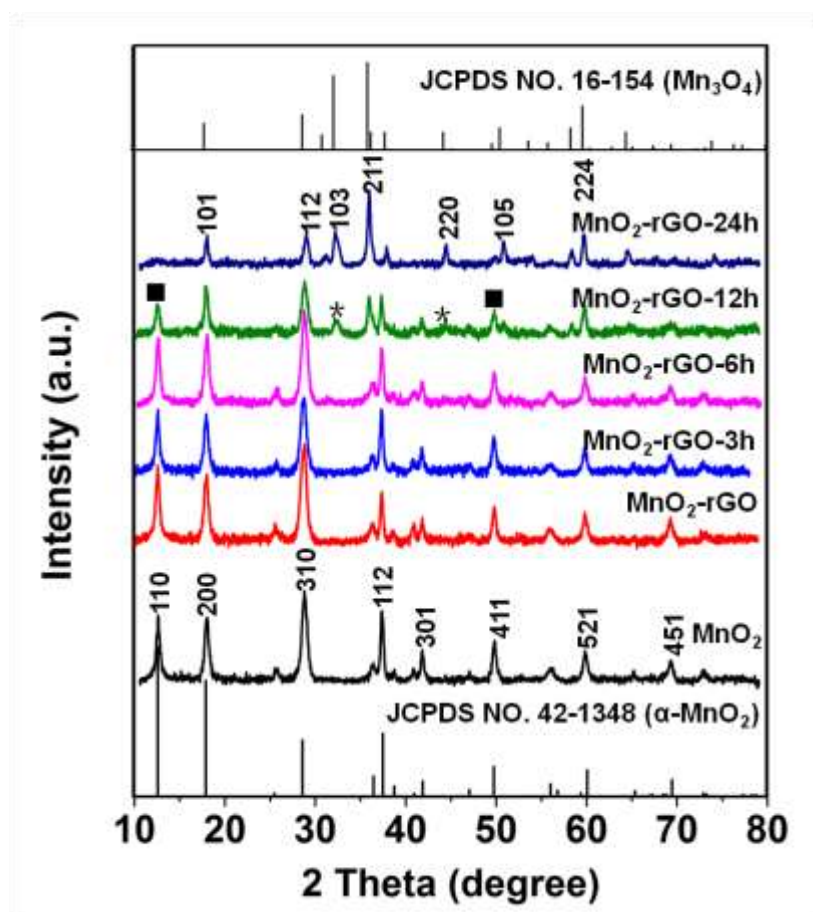


**Figure S5.** The XRD patterns of MnO<sub>2</sub>, MnO<sub>2</sub>/rGO, MnO<sub>2</sub>-rGO-3h (MnO<sub>2</sub>/pGO), MnO<sub>2</sub>-rGO-6h, MnO<sub>2</sub>-rGO-12h and MnO<sub>2</sub>-rGO-24h.

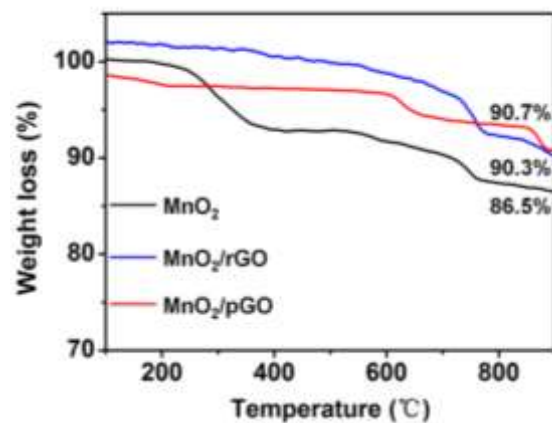


**Figure S6.** The TG curves of MnO<sub>2</sub>, MnO<sub>2</sub>/rGO and MnO<sub>2</sub>/pGO NWs.

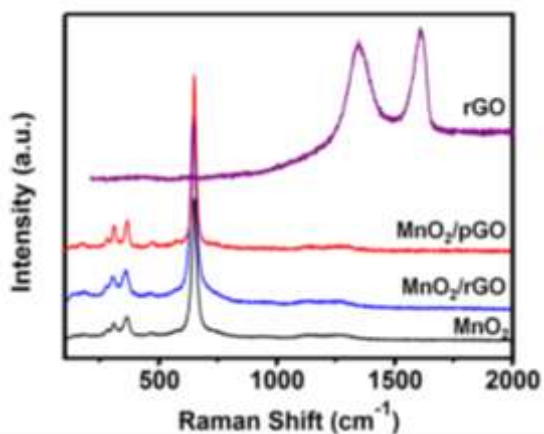


**Figure S7.** The Raman spectra of MnO<sub>2</sub>, MnO<sub>2</sub>/rGO, MnO<sub>2</sub>/pGO NWs and rGO, showing no obvious shifts among the MnO<sub>2</sub>, MnO<sub>2</sub>/rGO and MnO<sub>2</sub>/pGO NWs. Due to the small content of graphene (3.38 wt%), the D and G shifts between MnO<sub>2</sub>/rGO and MnO<sub>2</sub>/pGO NWs are not obvious.

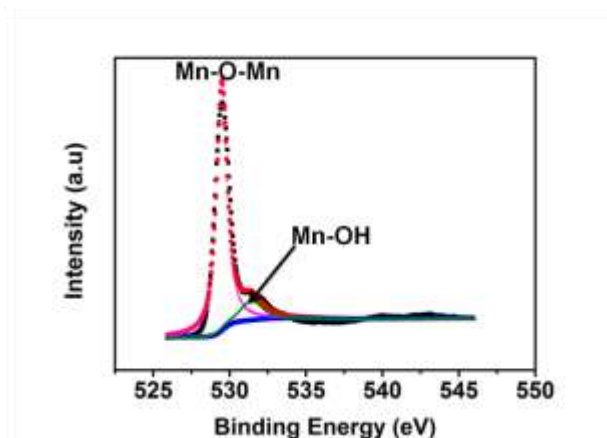


**Figure S8.** The O 1s XPS spectrum of MnO<sub>2</sub>. The O 1s core level spectrum is used to confirm the presence of oxygen vacancies in MnO<sub>2</sub>. The spectra can be fit with two components, which are related to the Mn-O-Mn bond (529.7 eV) of tetravalent oxide and the Mn-OH bond (531.43 eV) of hydrated trivalent oxide. Quantitative analysis shows that oxygen vacancies exist in MnO<sub>2</sub> because of the proportion of Mn<sup>3+</sup> in MnO<sub>2</sub> (13.84%).

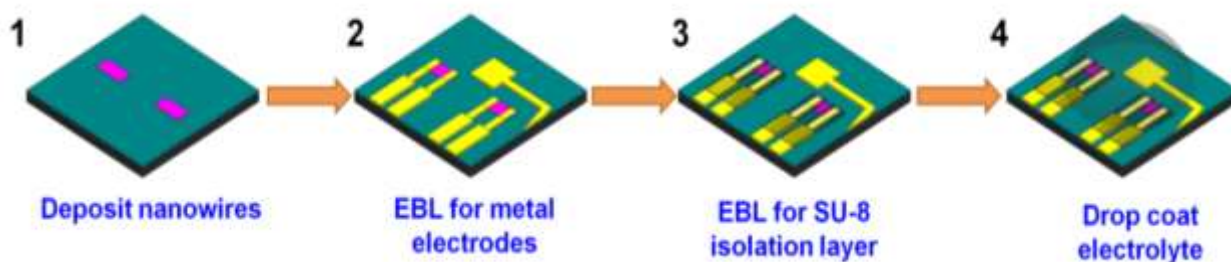


**Figure S9.** The fabrication processes of dropping electrolyte coating on a single-nanowire electrochemical device. The processes involve four steps. Step 1. EBL patterning of contact pads on a highly doped silicon wafer with 300 nm of SiO<sub>2</sub>, followed by developing, rinsing, Cr/Au (5/50 nm) deposition by thermal evaporation, and lift-off. The prepared MnO<sub>2</sub>, MnO<sub>2</sub>/rGO and MnO<sub>2</sub>/pGO NWs are deposited on the substrate. Step 2. Contacting the nanowires and contact pad with Cr/Au electrode through EBL patterning, developing, rinsing, Cr/Au (5/150 nm) deposition by thermal evaporation, and lift-off. Step 3. Using a probe station for air characterization to check the I-V cyclic voltammetry performance of the MnO<sub>2</sub>, MnO<sub>2</sub>/rGO and MnO<sub>2</sub>/pGO NWs. EBL patterning and developing of SU-8 2002 as an isolation layer of the gold

electrode to avoid leakage current. Step 4. Drop coating the KOH (6 mol/L) electrolyte on the nanowire and the counter electrode (Au), and test the performance of device.

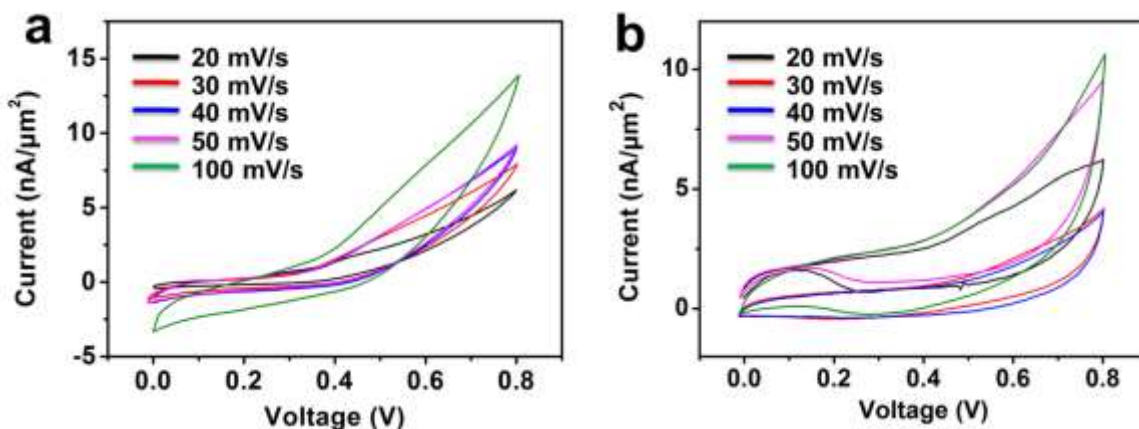


**Figure S10.** The CV curves at scan rates of 20, 30, 40, 50, and 100 mV/s for the as-prepared MnO<sub>2</sub> and MnO<sub>2</sub>/rGO single-nanowire electrochemical devices in 6 mol/L KOH.

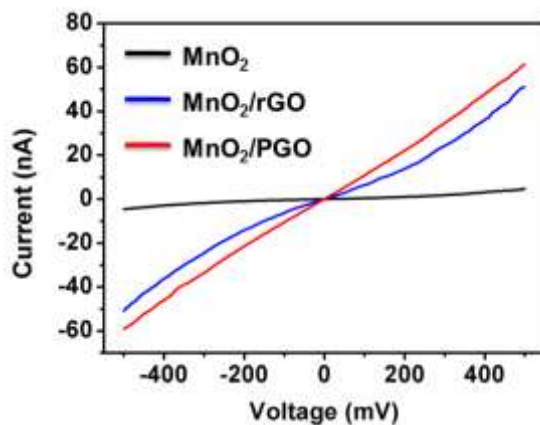


**Figure S11.** The single-nanowire transport properties of the MnO<sub>2</sub>, MnO<sub>2</sub>/rGO and MnO<sub>2</sub>/pGO NWs.

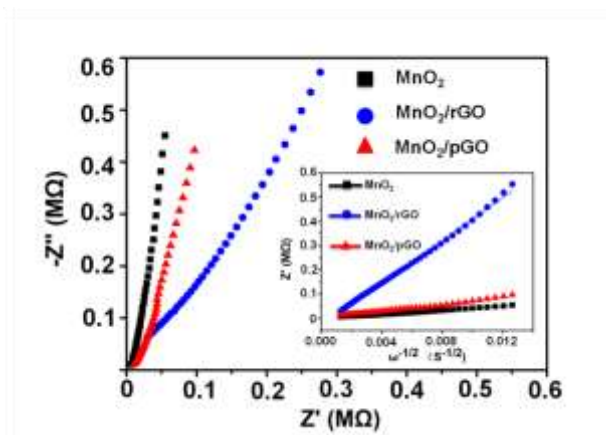


**Figure S12.** Nyquist plots of MnO<sub>2</sub>, MnO<sub>2</sub>/rGO and MnO<sub>2</sub>/pGO in a frequency regime from 1 to 100 kHz with a three-electrode system. The EIS measurements are performed in an aqueous solution of 6 mol/L KOH.

The ion diffusion coefficient can also be calculated using the following equation:

$$D = R^2 T^2 / 2A^2 n^4 F^4 C^2 \sigma^2$$

where  $R$  represents the gas constant,  $T$  represents the absolute temperature,  $A$  represents the surface area of the anode (cm<sup>2</sup>),  $n$  represents the number of electrons transferred in the half-reaction for the redox couple (2),  $F$  represents the Faraday constant,  $C$  represents the concentration of ions in the solid,  $D$  represents the diffusion coefficient (cm<sup>2</sup>/s), and  $\sigma$  represents the Warburg factor relative to  $Z_{re}$ . From the slope of the lines in the inset,  $\sigma$  can be obtained.

$$Z_{re} = R_D + R_L + \sigma \omega^{-1/2}$$

According to the linear fit, the slope of the real part of the complex impedance is versus  $\omega^{-1/2}$  (The response of AC impedance changes noisily when the frequency is below 10<sup>3</sup> Hz. Only impedance data in the frequency range of 10<sup>3</sup>~10<sup>6</sup> Hz is stable in the single-nanowire system.) at the potential of 0.3 V (vs HgCl/Hg) for MnO<sub>2</sub>, MnO<sub>2</sub>/rGO and MnO<sub>2</sub>/pGO NWs are 4.08×10<sup>6</sup>, 4.39×10<sup>7</sup> and 7.06×10<sup>6</sup>, respectively. The ions diffusion coefficients at room temperature are calculated to be 5.55×10<sup>-8</sup>, 5.21×10<sup>-9</sup> and 2.31×10<sup>-8</sup> cm<sup>2</sup>/s for the MnO<sub>2</sub>, MnO<sub>2</sub>/rGO and MnO<sub>2</sub>/pGO NW, respectively.

In general, the EIS contains  $R_{con}$ ,  $R_{ct}$ , and  $R_w$ . In this single-nanowire device system, the nanowire is surrounded by electrolyte, so ions are very easily transported to the interface of the active material. According to our understanding, the frequency of 10<sup>6</sup> Hz corresponds to  $R_{ct}$ ,

which may be due to the fast ion diffusion in our system.  $R_{\text{con}}$  and  $R_{\text{ct}}$  cannot be tested with Autolab 302N because of the upper frequency limitation. Only  $R_w$  can be calculated. In this way, the ion diffusion coefficients, which are calculated from the EIS, support our assertions in the manuscript.

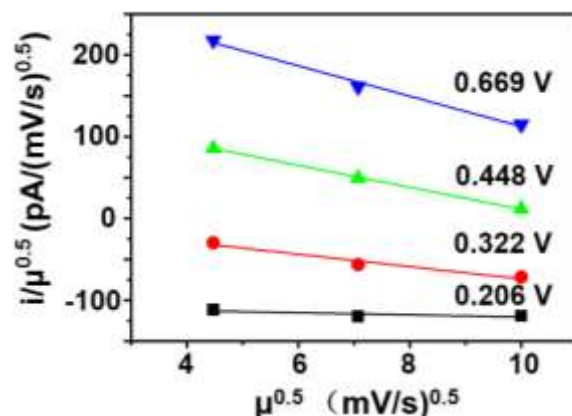


**Figure S13.** The plots of  $\mu^{0.5}$  vs  $i/\mu^{0.5}$  used for calculating constants  $k_1$  and  $k_2$  at different potentials from a variety of cathodic voltammetric sweeps. According to a power law relationship,  $I = k\mu$  for non-diffusion limited processes and  $i = k\mu^{0.5}$  for diffusion limited processes. Thus, total current  $i(V) = k_1\mu + k_2\mu^{0.5}$  and  $i(V)/\mu^{0.5} = k_1\mu^{0.5} + k_2$  at different potentials are calculated from cyclic voltammograms at different scan rates ranging from 20 to 500 mV/s. Plots of  $i/\mu^{0.5}$  vs  $\mu^{0.5}$  have been drawn at a variety of potentials. The  $k_1$  (slope) and  $k_2$  (intercept) are calculated from the straight line.

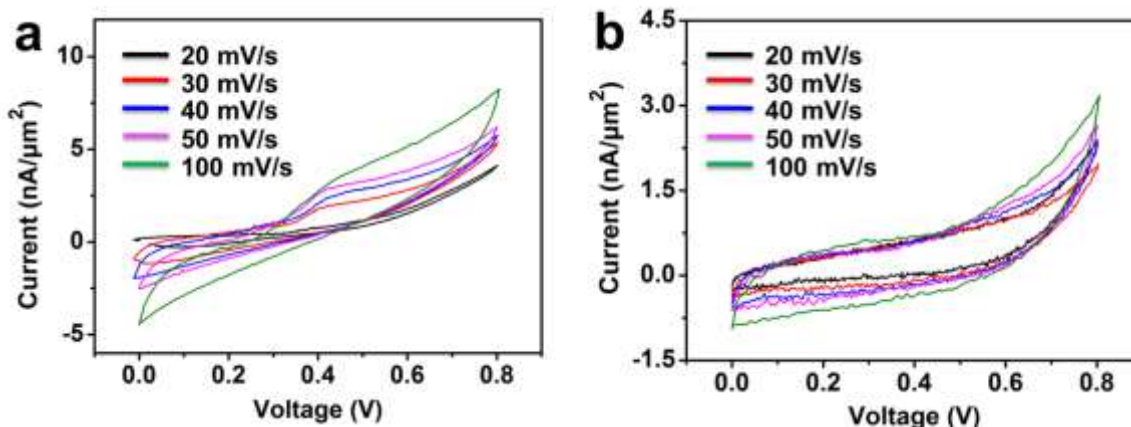


**Figure S14.** The CV curves at scan rates of 20, 30, 40, 50, and 100 mV/s for the as-prepared  $\text{MnO}_2$  and  $\text{MnO}_2/\text{rGO}$  symmetric single-nanowire electrochemical devices in 6 mol/L KOH.

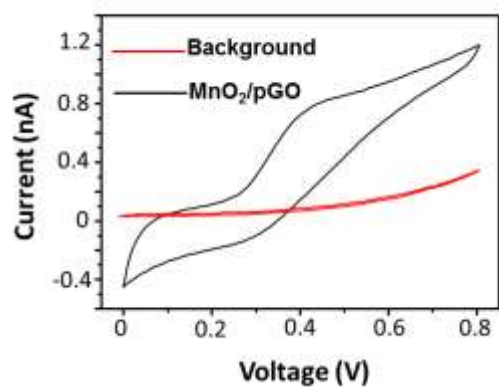


**Figure S15.** The CV curves at a scan rate of 100 mV/s for the MnO<sub>2</sub>/pGO symmetric single-nanowire electrochemical devices and background device in 6 mol/L KOH.